The in vitro and in vivo effects of [Cys25]hPTH(1-34) analogues

Chu Hyun Bae

Department of Medical Science

The Graduate School, Yonsei University

The in vitro and in vitro effects of [Cys25]hPTH(1-34) analogues

Directed by Professor Sung-Kil Lim

The Master's Thesis
submitted to the Department of Medical Science,
the Graduate School of Yonsei University
in partial fulfillment of the requirements for the degree of
Master of Medical Science

Chu Hyun Bae

June 2016

연세대학교
YONSEI UNIVERSITY

This certifies that the Master's Thesis of
Chu Hyun Bae is approved.

Thesis Supervisor: Sung-Kil Lim

Thesis Committee Member#1: Seong-Hwan Moon

Thesis Committee Member#2: Myung-Shik Lee

The Graduate School
Yonsei University

June 2016

ACKNOWLEDGEMENTS

Foremost, I would like to express my sincere gratitude to my advisor Prof. Sung-Kil Lim, for his patience, motivation, enthusiasm, and immense knowledge. His guidance helped me in all the time of research and writing of this thesis. I could not have imagined having a better advisor and mentor for my Master's degree study.

I would also like to thank the rest of my thesis committee, Prof. Je-Yong Choi, and Prof. Dong Min Shin, for their encouragement, and insightful comments.

My sincere thanks also go to Dr. Myeongmo Kang, Dr. Clara Yongjoo Park and Dr. Yu-Mi Yang and my fellow lab mates, Dongdong Zhang, Hee Jin Nam, and Bo Mi Park for the encouragement, stimulating discussions, and all the fun we have had in the last two years.

Last but not least, I would like to thank my family, my parents Kwang Soo Bae and Yong Eun Im, and my brother Dong Hyun Bae for supporting me throughout my life.

TABLE OF CONTENTS

ABSTRACT 1

I. INTRODUCTION 3

II. MATERIALS AND METHODS 6

1. Cell culture 6
2. Peptide synthesis 6
3. cAMP generation and wash out assay 6
4. pCRE-luciferase assay 7
5. Animal model 7
6. μCT analysis 7
7. Serum calcium analysis 8
8. Bone histomorphometry 8
9. Quantitative reverse transcription PCR (RT-PCR) 8
10. β-Arrestin dependent signals analysis 9
11. Statistical analysis 9

III. RESULTS 10

1. Gs protein-dependent signals 10
2. β-Arrestin dependent signals and RANKL/OPG mRNA expression 13

3. Acute effects of the peptides on serum calcium levels and bone mineral density 15
4. μCT analysis 18
5. Histomorphometric analysis 21

IV. DISCUSSION 23

V. CONCLUSION 26

REFERENCES 27

ABSTRACT (IN KOREAN) 35

LIST OF FIGURES

Figure 1. Cyclic AMP generation and its sustained response with hPTH(1-34) and the three derivative analogues.....12

Figure 2. Effects of hPTH(1-34) and three mutated peptides on arrestin-dependent signaling. 14

Figure 3. PTH and derivative analogues activity in vivo. 17

Figure 4. Changes in trabecular and cortical bone parameters assessed by μCT 19

LIST OF TABLES

Table 1. Trabecular and cortical structural parameter value I nC57BL/6 mice. 20

Table 2. Histomorphometry parameters about bone formation. 22

ABSTRACT

The in vitro and in vivo effects of [Cys25]hPTH(1-34) analogues

Chu Hyun Bae

Department of Medical Science
The Graduate School, Yonsei University

(Directed by Sung-Kil Lim)

Recently, an arginine (Arg)-to-cysteine (Cys) homozygous mutation at position 25 (R25C) in mature parathyroid hormone (PTH; 1-84) was reported in a Korean patient with hypoparathyroidism. To clarify whether the high bone mass phenotype observed in this patient is related to the hypoparathyroidism itself or a chronic elevation of mutant PTH, a series of *in vitro* and *in vivo* experiments were performed in MC3T3E1, ROS 17/2.8 and SAOS2 cells treated with hPTH(1-34), Cys^{25}hPTH(1-34), $Ala^{1}Cys^{25}$hPTH(1-34) and $Bpa^{1}Cys^{25}$hPTH(1-34). The synthesized peptides were then subcutaneously delivered to OVX mice as a daily single-dose regimen. Compared to hPTH(1-34) and $Ala^{1}Cys^{25}$hPTH(1-34), treatment with Cys^{25}hPTH(1-34) or $Bpa^{1}Cys^{25}$hPTH(1-34) revealed a decreased cAMP response and pCRE luciferase reporter activity. Although cAMP response was sustained with hPTH(1-34) in MC3T3E1 cells, such response was not observed when cells were treated with the three mutated peptides. Meanwhile, all PTH analogues exhibited ERK phosphorylation and cytoplasmic Ca^{++} signals comparable to hPTH(1-34). Compared to the control OVX mice, trabecular and cortical bone

parameters improved after 6 weeks of respective treatments as follows: hPTH(1-34)(80μg/kg) = $Ala^{1}Cys^{25}$hPTH(1-34)(80μg/kg) = Cys^{25}hPTH(1-34)(80μg/kg) > $Bpa^{1}Cys^{25}$hPTH(1-34)(80μg/kg) > hPTH(1-34)(40μg/kg). The increment in RANKL/OPG mRNA ratio after 6 hr treatment of Cys^{25}hPTH(1-34), $Ala^{1}Cys^{25}$hPTH(1-34) and $Bpa^{1}Cys^{25}$hPTH(1-34) was less than that was obtained after hPTH(1-34) treatment. In conclusion, the high bone mass phenotype observed in a Korean patient with hypoparathyrodism caused by an Arg to Cys mutation at the 25^{th} residue of mature PTH(1-84), may arise from direct and indirect effects exerted by the mutant PTH itself on bone. Cys^{25}PTH(1-34) could be a potential candidate as a second generation PTH analogue.

Key Words: PTH analogue, osteoporosis, bone anabolism

The in vitro and in vivo effects of [Cys25]hPTH(1-34) analogues

Chu Hyun Bae

Department of Medical Science
The Graduate School, Yonsei University

(Directed by Sung-Kil Lim)

I. INTRODUCTION

Parathyroid hormone (PTH), a polypeptide composed of 84 amino acids, plays a critical role in regulating of calcium and phosphate homeostasis and in remodeling bones.(1) Depending on its route of administration, PTH exerts differing effects *in vivo*, often referred to as the PTH paradox; an intermittent subcutaneous injection of PTH stimulates bone formation, while a continuous infusion causes hypercalcemia and induces loss in bone mass.(2) The bone anabolic effects by PTH from various mechanisms orchestrated in various cells. Remodeling-based bone formation by intermittent treatment of PTH is important, and modeling-based bone formation is also partially involved.(3) A low-dose intermittent treatment results in osteoblast differentiation, osteocyte activation, inhibited cell apoptosis, and suppressed sclerostin expression.(4) By stimulating aerobic glycolysis in osteoblasts via insulin-like growth factor signaling, PTH promotes bone anabolism.(5) Meanwhile, almost all of PTH's bone anabolic effects can be accomplished by its first 34 N-terminal amino acids.(6) Currently, teriparatide (PTH[1-34]), named Forteo, is commercially available as an anabolic agent for treating bone loss in the United States, although PTH(1-84) is also used for the treatment of osteoporosis in some countries.(7)

Previous studies have reported that residues 25-34 of PTH comprise the primary binding domain for the extracellular N domain of PTH/PTHrP receptor 1

(PTHR1).[8] The first two amino acids are also critical for receptor-binding interaction and cAMP generation.[9] Downstream signals of PTH are divided into a G-protein-dependent signaling and a β-arrestin-mediated signaling.[10] G-protein-dependent signaling is initiated by Gs and Gq11 coupling to the receptor and forming a functional complex upon binding of PTH to the receptor. The complex acts as a second messenger to activate downstream small G-protein regulators, such as adenyl cyclase/PKA, PLC/PKC, ion channel and Rho-GEF.[9,11] β-arrestin-mediated signaling also activates various signal molecules, including Src, MAPK, PI3K, to phosphatases like PP2A, phosphodiesterases like PDE4D, ubiquitin ligases like Mdm2, small G-protein regulator Ral-GDS and transcriptional regulator IkB.[12-14] Recently, Kobilka BK et al. proposed that PTH/PTHrP receptor exists in two different conformations, R^0 and RG.[15] Interestingly, the authors highlighted that PTHrP has a high affinity for the RG form, yet PTH binds with a greater selectivity to the R^0 form.[16,17] Furthermore, if PTH binds with the R^0 form, endocytosis is induced for continuous cAMP generation in early endosomes, called a sustained response.[18] Accordingly, development of new, biased PTH analogue has been attempted for use in increasing bone mineral densities (BMD), while minimizing side-effects of hypercalcemia and cortical porosity by transforming PTH signal transduction.

It has been reported that daily, single subcutaneous injection of hPTH(1-34) significantly increases spinal BMD, but not femoral BMD until at least 9 mo after treatment.[19] Also, the rates of BMD increase and fracture prevention were not found to be greater than those achieved with alendronate.[20] In conjunction, hPTH(1-34) increased cortical porosity, which significantly weakens bone strength.[21] To overcome these problems, PTHrP-based Abaloparatide has been developed as a pure agonist, and has completed phase III clinical trials.[22] Teribone, was also developed and introduced in the Japanese market as a once weekly agent.[23] Although the drug effects were reported not to be reduced, the neutralizing antibody was developed in many patients treated with Abaloparatide, and the side effects such as hypercalcemia episode and hypotension followed by discontinuation were frequent in patients with

Teribone.[22,24,25] Therefore, more studies for development of new PTH derivatives that are safe, effective, and convenient are required.

Recently, Lee et al. reported on hypoparathyroidism in a patient caused by a substitution of the 25th residue of hPTH(1-84) from Arg to Cys.[26] Interestingly, this patient exhibited a notable increase in the level of serum PTH measured via an assay that utilized residue sequences 1-3 and 35-84 as an epitope for antibodies. Since the residues 25-34 of hPTH(1-84) is the primary receptor-binding domain, the Arg-to-Cys substitution at the 25th residue of Cys^{25}hPTH(1-34) exhibited a three-times weaker receptor binding and cAMP generation than those of the wild-type hPTH(1-34) activity.[26] When administrating Cys^{25}hPTH(1-34) via IV infusion for 4 days, hypocalcemia and hyperphosphatemia developed, and reductions in 1 alpha hydroxylase and TRPV5 expression were confirmed in mice.[26] Interestingly, BMD in the aforementioned patient was significantly high (personal communication). High BMD in patients with hypoparathyroidism has been already reported before; it has also been reported in Korean patients.[27] Thus, in this study, we synthesized Cys^{25}hPTH(1-34) analogues and injected them subcutaneously and intermittently as a daily single dose in OVX mice to 1) identify whether the high BMD observed in this patient is caused by hypoparathyroidism itself or long-term elevation of mutant hPTH, 2) investigate which signaling pathways are activated, and 3) elucidate the significance of the first amino acid of Cys^{25}hPTH(1-34) in its role of serum calcium and BMD modulation.

II. MATERIALS AND METHODS

1. Cell culture

Mouse pre-osteoblast MC3T3-E1 cells were maintained in Alpha Minimum Essential Medium (alpha MEM) containing 10% FBS and 1% penicillin-streptomycin. ROS 17/2.8 rat osteosarcoma cells were cultured in Dulbecco's modified Eagle's medium (DMEM) containing 10% FBS and 1% penicillin-streptomycin. SAOS2 cells were maintained in McCoy's 5A containing 15% FBS and 1% penicillin-streptomycin. All cell lines were incubated at 37°C with 5% CO_2. All used cell in experiments were less than 15 passages.

2. Peptide synthesis

Peptides were synthesized by Fmoc SPPS (solid phase peptide synthesis) using ASP48S (Peptron Inc, Taejeon, South Korea). Human PTH derivatives used included hPTH(1-34), Cys^{25}hPTH(1-34), $Ala^{1}Cys^{25}$hPTH(1-34) and $Bpa^{1}Cys^{25}$hPTH(1-34). Peptides were purified using reverse phase HPLC on a Vydac Everest C18 column (250 mm x 22 mm, 10μm). The solution was eluted with a water-acetonitrile linear gradient (3-40% [v/v] of acetonitrile) containing 0.1% (v/v) trifluoroacetic acid. Molecular weight of the purified peptide was confirmed using LC/MS (Agilent HP1100 series).

3. cAMP generation and wash out assay

cAMP generation and wash out assay were proceeded as previously described.[19] Briefly, the peptides were added to MC3T3E1 cells in cAMP buffer (0.1% BSA, 20mM HEPES, 20μg/ml ascorbic acid in DMEM media). Samples were incubated for 20 minutes at 37°C, and the media was replaced with 1ml of 50mM HCl. The same procedure was performed for the washout assay with 1 x 10^{-7}M of the peptides. After the incubation at 37°C, cAMP buffer was replaced with 2mM IBMX and incubated at 37°C. Intra-cellular cAMP was quantified usting Cayman cyclic AMP EIA kit.

4. pCRE-luciferase assay

SAOS2 cells, plated in 6-well plates (~0.3x10^6/well), were transfected with TransIT-2020 transfection reagent (Mirus), and cultured over 2 days to ensure the expression of pCRE-luciferase. Luciferase activity was measured 8 hr after the treatment with the peptides.

5. Animal model

Female virgin C57BL/6J mice (**Japan SLC, Inc, Shizuoka, Japan**) underwent bilateral sham or ovariectomy (OVX) operation at 8 weeks of age. All mice were maintained for 5 we after OVX operation to induce bone loss. Operated mice were subcutaneously injected with the peptides upon randomly assigned group (n=7/group). Injected dosages of hPTH(1-34) were 40μg/kg and 80μg/kg, while the other peptides were dosed at 80μg/kg. The sham group and one OVX-operated group were injected with saline. All groups were injected for 5 days per week over 6 weeks. At the end of the injection period, mice blood samples were collected at 0, 1, 2 and 3 hours after subcutaneous injections to measure serum calcium levels. Tibia, femur and spinal cord were also collected for μCT analysis. Animal protocols were carefully reviewed and approved by Yonsei Biomedical Research Institute (Seoul, Korea), based on the guidelines for the care and use of laboratory animals (National Research Council, USA).

6. μCT analysis

Mouse tibiae were imaged with a high resolution system (SkyScan 1076). Using Skyscan CT analyzer software (Nrecon for section forming and Ctan/Ctvo1 for analyzing), several micro-parameters in mouse right tibia, trabecular and cortical bones were quantified.

7. Serum calcium analysis

DRY- CHEM 4000i parameters were used to measure calcium levels in mouse blood serum with FUJIFILM Corporation slides (FUJUFILM, FUJU DRI-CHEM SLIDE, Ca-PIII). Blood samples were incubated for 30-60 minutes at room temperature and centrifuged at 500rpm for 10 minutes.

8. Bone histomorphometry

Mice were intraperitoneally injected with 10 mg/kg calcein two and seven days before they were sacrificed and subjected to dynamic histomorphometry. Undecalcified distal femurs were embedded in methyl methacrylate as previously described.[28] 6 μm-thick sagittal sections were analyzed for bone formation rate (BFR), mineral apposition rate (MAR), and mineralizing surface over bone surface (MS/BS) of trabecular and cortical bone. Histomorphometrical analyses were performed with Bioquant Osteo II (Bio-Quant, Inc., Nashvile, TN). For samples with only single labels, MAR was assigned with a minimum value of 0.1 μm/d.[29] All bone histomorphometric nomenclatures follow the guidelines of the ASBMR.[29]

9. Quantitative reverse transcriptional PCR (RT-PCR)

MC3T3-E1 cells were treated with each peptide at $1x10^{-8}$M for 6 hr. After the treatment, mRNA was extracted with TRIzol and used to synthesize its cDNA. The following primers were used : 5'-CAT TTG CAC ACC TCA CCA TCA AT-3' (forward) and 5'-GTC TGT AGG TAC GCT TCC CG-3' (reverse) (mouse RANKL); 5'-ACC CAG AAA CTG GTC ATC AGC-3' (forward) and 5'CTG CAA TAC ACA CAC TCATCA CT-3' (reverse) (mouse OPG); 5'-GCT ACA GCT TCA CCA CCA CAG-3' (forward) and 5'-GGT CTT TAC GGA TGT CAA CGT C-3' (reverse) (mouse β-actin).

10. β-Arrestin dependent signals analysis

The method of $[Ca^{++}]_i$ imaging has been described previously.[30] Briefly,

MC3T3E1 cells were loaded with 0.05% pluronic F-127 and 5μM Fura-2/AM (Teflabs Inc., Austin, TX) for 1 hour in physiologic salt buffer. Fura-2 fluorescence was measured with Molecular Devices (Downingtown, PA) imaging system. The emitted fluorescence was detected with a charge-coupled camera device (Photometrics, Tucson, AZ) attached to an inverted microscope. Fluorescence images were analyzed using MetaFluor software (Molecular Devices). For western blot analysis, MC3T3E-1 cells were introduced with 10^{-8}M peptides for 5, 10 and 20 min. Primary antibodies were probed for phospho-ERK (Phospho-p44/42 MAPK (Erk1/2)(Thr202/Tyr204) Antibody, Cell Signaling), ERK (p44/42 MAPK (Erk1/2) Antibody, Cell Signaling) and actin (Actin (C-2):sc-5432, Santa Cruz).

11. Statistical analysis

All collected data sets were analyzed using Excel 2010 (Microsoft Corp. Redmond, WA, USA) and Graphpad Prism 5 (Graphpad software Inc., La Jolla, CA, USA), presented as mean ± S.D. Paired data sets were computed by Student's t test. $P<0.05$ was considered statistically significant.

III. RESULTS

1. Gs protein-dependent signals

We examined the effect of the PTH derivatives in activating Gs protein-dependent signaling pathway of PTH in ROS 17/2.8 cells. Cells treated with control hPTH(1-34) exhibited a dose-dependent effect on cAMP generation, while the mutant Cys^{25}hPTH(1-34), in which the amino acid at position 25 was substituted with a cysteine residue, showed a reduced generation ability, especially at a concentration of 10^{-8}M, compared to the control hPTH(1-34). However, $Ala^{1}Cys^{25}$hPTH(1-34), in which the normal amino acid at position 1 was also substituted with an alanine residue, was able to rescue the cAMP generation potency in ROS 17/2.8 cells. $Bpa^{1}Cys^{25}$hPTH(1-34) exhibited the lowest cAMP generation activity amongst the PTH derivatives (Fig. 1A; *p value <0.05, **p value <0.01 versus hPTH(1-34)). The first residue in Cys^{25} mutants could also affect cAMP generation. After an induction of a transient expression of cAMP response element (CRE) reporter DNA in SAOS2 cells, the activity of the reporter responding to each peptide was measured. $Ala^{1}Cys^{25}$hPTH(1-34) revealed a reporter activity similar to wild-type hPTH(1-34). Reporter activity was reduced in Cys^{25}hPTH(1-34) and $Bpa^{1}Cys^{25}$hPTH(1-34) (Fig. 1B; *p value <0.05 versus hPTH(1-34)). Additionally, we conducted a wash-out assay with hPTH(1-34) and Cys^{25} mutated PTHs to monitor changes in intracellular cAMP concentration after PTH stimulation in ROS17/2.8 cells. After 10 min of 10^{-7}M of PTH, we measured the concentration of cAMP using ELISA. The control group, treated with hPTH(1-34), showed a sustained effect consistent with what Lee et al. had previously reported, while the other peptides with a Cys^{25} mutation could not lead to responses as sustained as the control group, regardless of the substitution of the first amino acid (Fig. 1C; *p value <0.05 versus hPTH[1-34]). Since all three mutant peptides showed no significant

differences, we concluded that the first amino acid substitution in Cys^{25}hPTH(1-34) does not affect the sustained effect of cAMP generation. As a result, when the Arg at position 25 was mutated to Cys in hPTH(1-34), the sustained cAMP response of hPTH(1-34) disappeared.

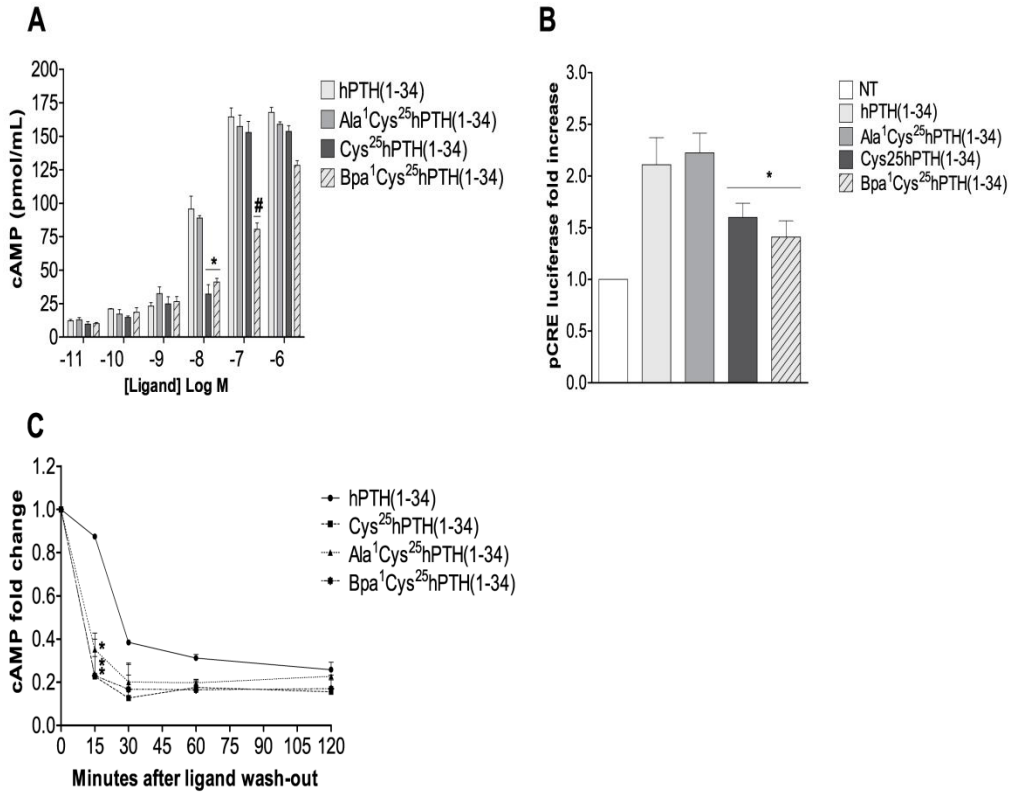

Figure 1. Cyclic AMP generation and its sustained response with hPTH(1-34) and the three derivative analogues. (A) Ligand-induced cAMP potency was detected in ROS 17/2.8 rat osteosarcoma cells. The cells were plated in 24-well plates and treated with 10^{-6} to 10^{-12}M of hPTH(1-34), Cys^{25}hPTH(1-34), $Ala^{1}Cys^{25}$hPTH(1-34) or $Bpa^{1}Cys^{25}$hPTH(1-34). The peak responses were measured at 20 min after ligand addition. (B) Cyclic AMP-mediated CRE (cAMP response element) response assay was measured in SAOS2 cells expressing pCRE-luciferase. SAOS2 cells with transient expression of pCRE-luciferase were treated with 10^{-8}M of hPTH(1-34) or the three PTH analogues. The peak luciferase was assessed with a plate reader at 8 hours after ligand addition. (C) cAMP sustained response after the ligands were washed out was also assessed in

ROS 17/2.8 cells. 2mM IBMX was added for 2-5 min prior to the ligand treatment. 10^{-6}M of each peptide was added for 10 min and washed twice with a buffer without IBMX. Then, cells were incubated for 15, 30, 60 and 120 min in a buffer containing IBMX. Data sets are presented in means ±S.D. of 3 to 5 experiments (A, B, C), each performed in duplicates. *: $p<0.05$ (versus hPTH(1-34)); **: $p<0.01$ (versus hPTH(1-34)).

2. β-Arrestin dependent signals and RANKL/OPG mRNA expression

All peptides were able to induce ERK phosphorylation 5 min after the signal activated by the peptides, and sustained until 20 min post-activation (Fig. 2A). Cysteine mutated PTHs were able to result in a slightly higher ERK phosphorylation, but $Bpa^{1}Cys^{25}$hPTH(1-34) showed less phosphorylation level, compared to the other mutant peptides. In order to measure cytoplasmic calcium level, MC3T3E1 cells were treated with 10^{-8}M of ligands. We noticed that the control and the modified peptides induced similar increases in cytoplasmic calcium levels (Fig. 2B; *p value<0.05 versus ATP). Therefore, as Lee et al. reported, we confirmed that hPTH(1-34) and the mutant PTH peptides similarly contributed to β-arrestin-mediated cytoplasmic calcium regulation.

The mRNA expression levels of RANKL and OPG were measured after treatment of MC3T3E1 cells with the peptides. Cells without any peptide treatments expressed low or basal levels of RANKL and OPG mRNAs. However, the mRNA expression level of RANKL increased significantly upon 6-hour hPTH treatment (Fig. 2C). The following it the rank of the potency of each ligand: $Ala^{1}Cys^{25}$hPTH(1-34) > Cys^{25}hPTH(1-34) > $Bpa^{1}Cys^{25}$hPTH(1-34). OPG expression levels were not noticeably changed when cells were treated with hPTH(1-34) but increased with Cys^{25} mutant PTHs. Upon quantifying band densities, RANKL/OPG mRNA expression ratio significantly increased after treatment with hPTH(1-34), although it was not increased after treatment with Cys^{25} mutant PTHs.

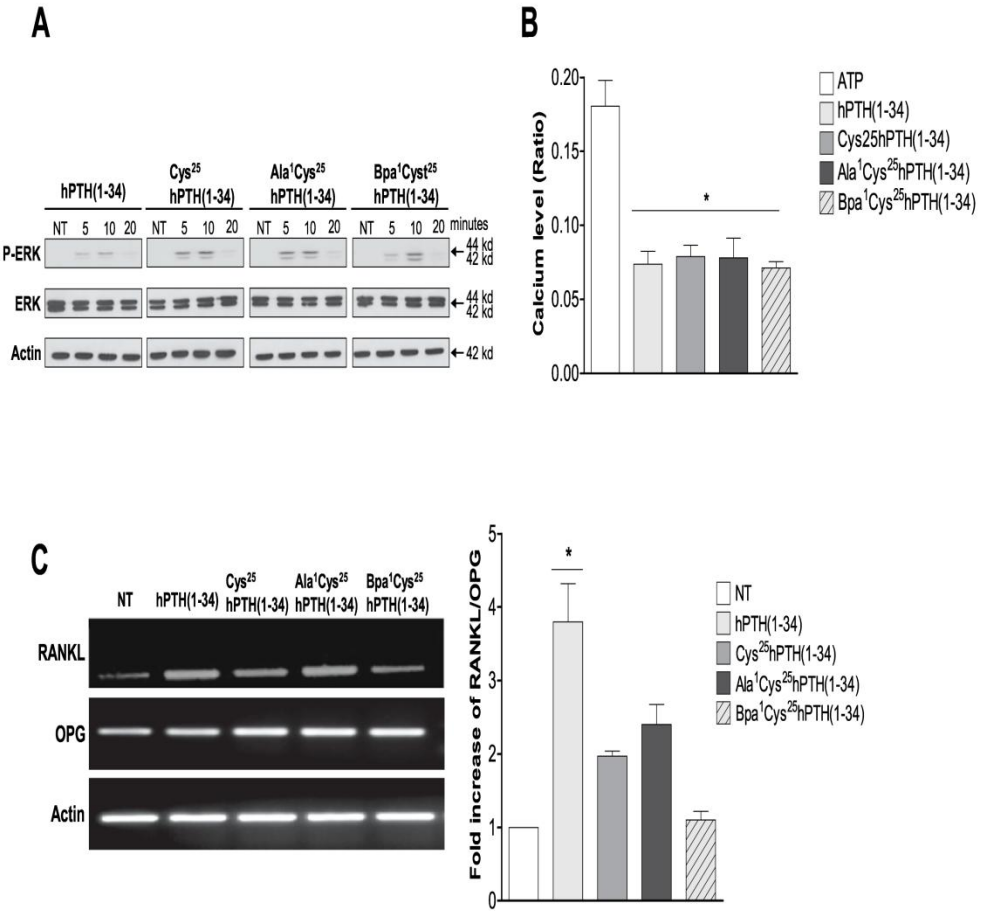

Figure 2. Effects of hPTH(1-34) and three mutated peptides on arrestin-dependent signaling. (A) MC3T3E1 pre-osteoblast cells were treated with hPTH or its analogues (10^{-9}M) for 5, 10 and 20 min. Cellular proteins from the whole cell lysates were isolated to detect ERK phosphorylation using phosphorylated or total ERK1/2 antibody. hPTH(1-34) and its analogues induced ERK1/2 phosphorylation from 5 minutes after the treatment. (B) Ligand-induced Ca^{++} responses in MC3T3E1

cells. Cells were attached to a cover glass in a 35-mm dish. 10^{-8}M of the peptides were added and loaded with 5μM Fura-2/AM and 0.05% pluronic F-127 for 60 min after 24-48 hr. The fluorescence reading were analyzed using MetaFluor software. (C) mRNA expressions of RANKL, OPG and β-actin and the ratio of RANKL/OPG mRNA. mRNA expression levels of RANKL, OPG and β-actin in MC3T3E1 cells were assessed by RT-PCR. 10^{-8}M of the ligands were introduced in normal cell culture media without FBS, and the cells were incubated for 6 hr. The graph represents RANKL/OPG ratio. All the data were analyzed using Multi-gauge V3.0 software. Representative data sets are presented as means ±S.D. of 3 to 5 experiments (A, B, C), each performed in triplicates. *: $p<0.05$ (versus ATP)

3. Acute effects of the peptides on serum calcium levels and bone mineral density

We noticed an increase in serum calcium level in the control hPTH(1-34) group and the experimental groups, with the level reaching 5~10% peak increase at 1 hr post injection (Fig. 3A). Amongst the mutant peptides groups, mice subjected to $Ala^{1}Cys^{25}$hPTH(1-34) injection exerted the highest increase in calcium levels (*p value <0.05 versus OVX+saline; n = 6~7). Only the group of mice injected with 40μg/kg of hPTH(1-34) showed a difference in calcium levels, probably due to a lower dosage than the other mice.

BMD of left femurs was quantified using PIXImus software (Fig. 3B). The average BMDs of the sham operation and the OVX+saline group were 0.098g/cm^2 and 0.089g/cm^2, respectively, which were markedly reduced. While no significant increase in BMD level was detected in the

group with 40μg/kg of hPTH(1-34), the BMD increased up to 0.100g/cm^2 in the group which received 80μg/kg of hPTH(1-34). The other peptide groups also exhibited significant increases in BMD. Compared with the OVX group, both the sham and mutant peptide groups showed statistically significant higher BMDs (*p value <0.05 versus OVX+saline; n = 5~6). Thus, we suspected that daily single injections of hPTH or its derivatives must contribute to the bone anabolic effect.

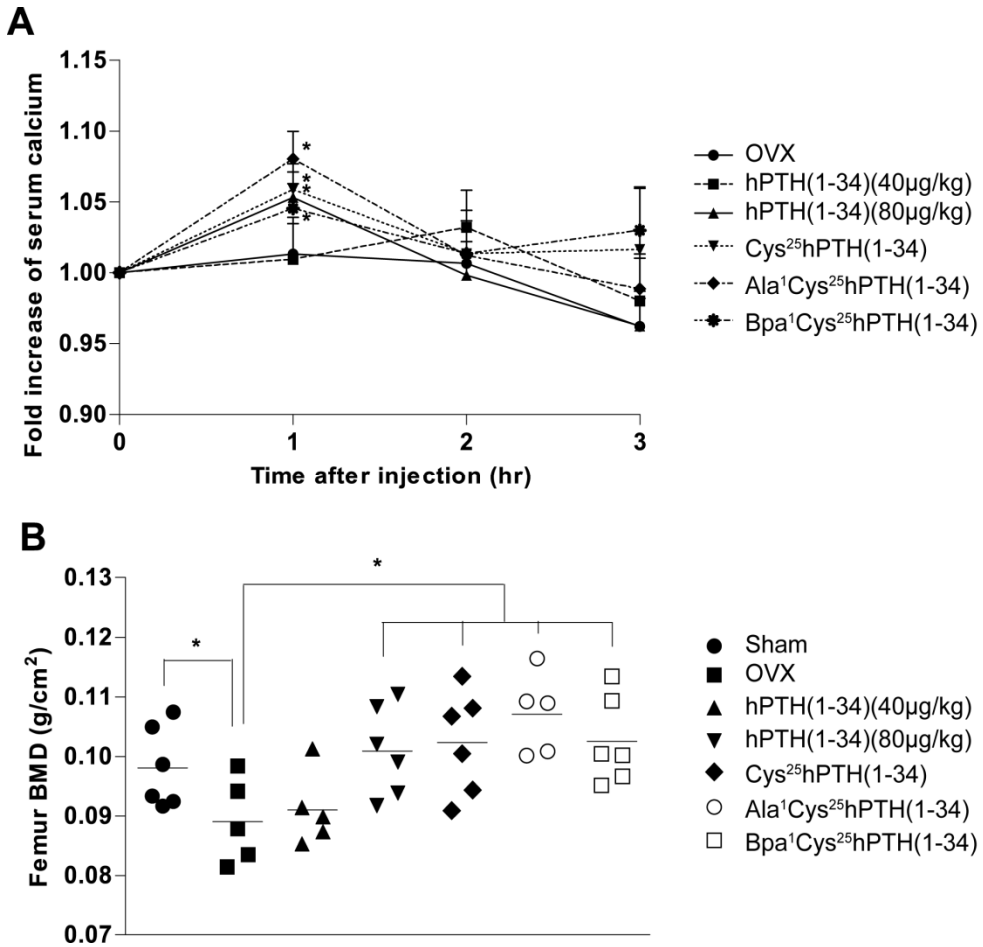

Figure 3. PTH and derivative analogues activity *in vivo*. (A) Vehicle (saline) and the PTH analogues were subcutaneously injected into C57BL/6 mice 6 we post OVX or sham operation. Acute injection were performed with 40μg/kg of hPTH(1-34), or 80μg/kg of hPTH(1-34), Cys^{25}hPTH(1-34), $Ala^{1}Cys^{25}$hPTH(1-34) or $Bpa^{1}Cys^{25}$hPTH(1-34). Blood serum was isolated from the total blood samples, extracted 0, 1, 2 and 3 hr after the injections. (B) Bone mineral density (BMD) of mice femurs was measured with Lunar PIXImus 2 densitometer and further analyzed using Lunar PIXImus 2 software (GE medical systems). Data are presented as means ±S.D. from a single experiment in 5 to 7 mice (A, B) per group. *: $p<0.05$ (versus OVX+ saline group

4. μCT analysis

μCT analysis assessed various bone parameters of the right tibia. In the representative images, we noticed that the OVX group had a visual trabecular and a cortical bone loss (Fig. 4A). Groups that received 80μg/kg of hPTH(1-34), Cys^{25}hPTH(1-34) and $Ala^{1}Cys^{25}$hPTH(1-34) had enhanced its trabecular and cortical bone parameters, while the other groups, 40μg/kg of hPTH(1-34) and $Bpa^{1}Cys^{25}$hPTH(1-34) remained the same with no significant differences. (Fig. 4B, C; Table 1). In particular, the analysis showed that there was a significant reduction of the percent bone volume tissue-volume (BV/TV) ratio from trabecular bone parameters in the OVX group, compared to the sham group; significant increases in these values were also confirmed in the mutant peptide groups. Also, the OVX group had the highest trabecular separation (Tb.Sp) and bone-surface/volume ratio (BS/BV), while the ratio of the other peptide groups tended to be lower. $Bpa^{1}Cys^{25}$hPTH(1-34) injected mice showed no noticeable difference. Cortical bone parameters also showed meaningful results: OVX group mice had the lowest cortical bone volume and cross-sectional thickness. The 80μg/kg hPTH(1-34) group and all mutant peptide groups recovered the values, but the 40μg/kg hPTH(1-34) mice did not. Moreover, the OVX group had the highest cortical BS/BV, while the other peptide groups showed a lower value. Conclusively, 80μg/kg hPTH(1-34), Cys^{25}hPTH(1-34) and $Ala^{1}Cys^{25}$hPTH(1-34) peptides affect bone anabolic effects, although 40μg/kg hPTH(1-34) and $Bpa^{1}Cys^{25}$hPTH(1-34) may not as much (*p value <0.05, #p value <0.01 versus OVX+saline; n = 5~8).

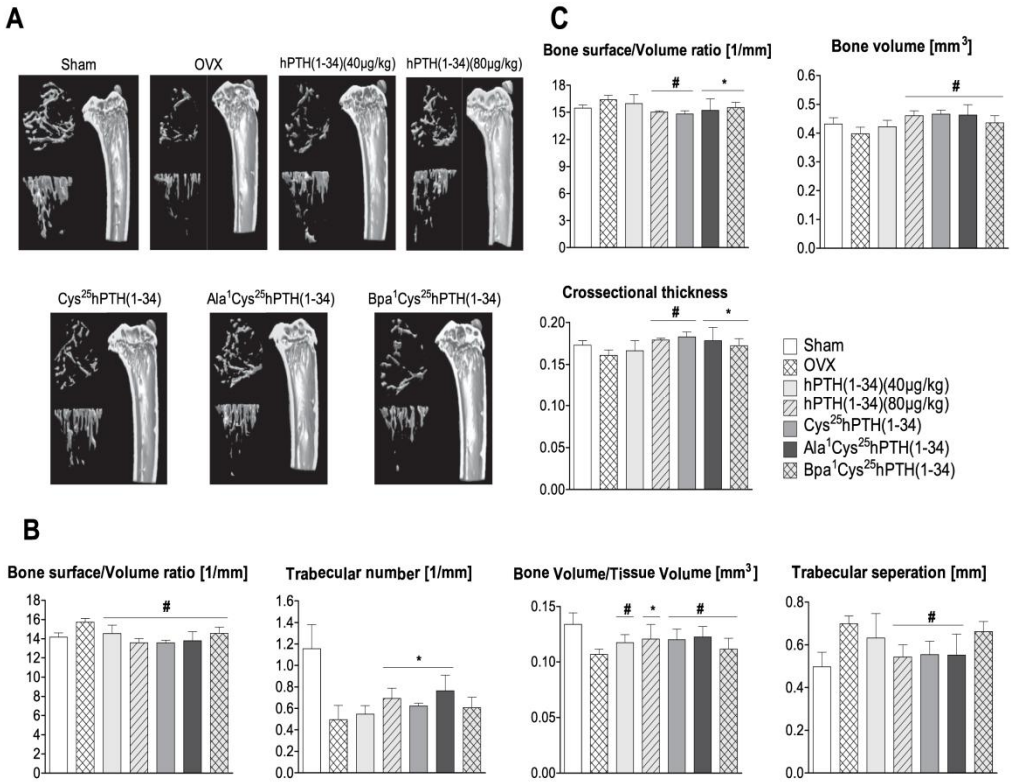

Figure 4. Changes in trabecular and cortical bone parameters assessed by μCT. (A) Representative μCT images of trabecular bone. Transverse and longitudinal views are shown on the left. Longitudinal images are shown on the right. (B) Tibia trabecular bone parameters were measured by μCT. Trabecular number [1/mm], Bone Volume/Tissue Volume [mm^3], Trabecular separation [mm] and Bone surface/Volume ratio [1/mm] are depicted in the figure, and other parameters are shown in Table 1. (C) Tibia cortical bone parameters. Bone volume [mm^3], Bone surface/Volume ratio [1/mm] and cross-sectional thickness arez shown, and other parameters are shown in Table 1. Data are presented as means ±S.D. from a single experiment, from 5 to 8 mice (A, B, C) per group. *: $p<0.05$ (versus OVX+saline group); #: $p<0.01$ (versus OVX+saline group).

Table 1. Trabecular and cortical structural parameter values in C57BL/6 mice

Trabecular bone	Sham	OVX	hPTH(1-34) (40μg/kg)	hPTH(1-34) (80μg/kg)	Cys^{25} hPTH(1-34)	$Ala^{1}Cys^{25}$ hPTH(1-34)	$Bpa^{1}Cys^{25}$ hPTH(1-34)
Tissue volume[mm^3]	14.77 ± 0.80	15.42 ± 0.62	16.14 ± 0.56*	17.40 ± 2.34	16.80 ± 1.43*	16.80 ± 0.82#	16.60 ± 0.71#
Bone volume[mm^3]	1.98 ± 0.10	1.64 ± 0.09	1.89 ± 0.09#	2.04 ± 0.07#	2.02 ± 0.04#	2.06 ± 0.15#	1.85 ± 0.12#
Percent bone volume[%]	13.42 ± 1.04	10.67 ± 0.49	11.75 ± 0.73#	12.22 ± 1.31*	12.07 ± 0.95#	12.28 ± 0.93#	11.17 ± 0.99
Bone surface[mm^2]	28.01 ± 1.31	25.88 ± 1.41	27.49 ± 0.65*	27.68 ± 0.96*	27.36 ± 0.82*	28.28 ± 1.03#	26.87 ± 0.89
Bone surface/Volume ratio[1/mm]	14.18 ± 0.44	15.74 ± 0.38	14.55 ± 0.87#	13.58 ± 0.46#	13.57 ± 0.28#	13.78 ± 0.94#	14.56 ± 0.65#
Bone surface density[1/mm]	1.90 ± 0.15	1.68 ± 0.07	1.70 ± 0.04	1.66 ± 0.19	1.64 ± 0.15	1.689 ± 0.06	1.62 ± 0.09
Trabecular thickness[mm]	0.074 ± 0.002	0.075 ± 0.002	0.073 ± 0.001	0.074 ± 0.002	0.073 ± 0.001	0.073 ± 0.002	0.073 ± 0.002
Trabecular number[1/mm]	1.16 ± 0.22	0.50 ± 0.13	0.55 ± 0.08	0.69 ± 0.10*	0.62 ± 0.03*	0.76 ± 0.15*	0.61 ± 0.09
Trabecular separation[mm]	0.50 ± 0.07	0.70 ± 0.04	0.60 ± 0.11	0.54 ± 0.06#	0.55 ± 0.06#	0.55 ± 0.10#	0.66 ± 0.05
Trabecular pattern factor[mm]	13.70 ± 2.25	16.86 ± 2.95	18.36 ± 1.62	18.22 ± 1.29	19.00 ± 1.68	18.18 ± 2.16	16.95 ± 1.58
Structure model index.	2.39 ± 0.11	2.54 ± 0.10	2.64 ± 0.08*	2.66 ± 0.06*	2.68 ± 0.05#	2.67 ± 0.10*	2.54 ± 0.12
Connectivity	59.00 ± 11.88	45.86 ± 17.28	46.86 ± 12.60	54.86 ± 15.12	41.43 ± 10.33	52.57 ± 11.63	44.71 ± 11.06
Connectivity density[1/mm^3]	27.47 ± 4.67	21.85 ± 6.84	21.68 ± 5.71	26.44 ± 6.38	20.24 ± 4.87	24.45 ± 5.59	21.44 ± 5.34
Degree of anisotropy	0.66 ± 0.03	0.65 ± 0.06	0.64 ± 0.03	0.63 ± 0.03	0.66 ± 0.02	0.60 ± 0.07	0.624 ± 0.06
Cortical bone	Sham	OVX	hPTH(1-34) (40μg/kg)	hPTH(1-34) (80μg/kg)	Cys^{25} hPTH(1-34)	$Ala^{1}Cys^{25}$ hPTH(1-34)	$Bpa^{1}Cys^{25}$ hPTH(1-34)
Tissue volume[mm^3]	2.54 ± 0.44	2.30 ± 0.33	2.13 ± 0.27	2.43 ± 0.44	2.35 ± 0.25	2.46 ± 0.35	2.46 ± 0.14
Bone volume[mm^3]	0.43 ± 0.02	0.40 ± 0.02	0.42 ± 0.02	0.46 ± 0.02#	0.47 ± 0.01#	0.46 ± 0.04#	0.44 ± 0.02#
Percent bone volume[%]	17.38 ± 2.48	17.52 ± 1.96	20.10 ± 2.64	19.52 ± 3.43	19.99 ± 2.06*	19.04 2.42±	17.81 ± 1.73
Bone surface[mm^2]	6.67 ± 0.20	6.52 ± 0.38	6.75 ± 0.42	6.93 ± 0.22*	6.91 ± 0.21*	7.01 ± 0.29*	6.76 ± 0.23
Bone surface/volume ratio [1/mm]	15.47 ± 0.37	16.38 ± 0.51	15.99 ± 0.97	15.03 ± 0.16#	14.83 ± 0.36#	15.22 ± 1.28*	15.52 ± 0.58*
Bone surface density[1/mm]	2.69 ± 0.39	2.87 ± 0.29	3.20 ± 0.29	2.93 ± 0.50	2.96 ± 0.26	2.89 ± 0.37	2.76 ± 0.18
Cross-sectional thickness[mm]	0.17 ± 0.01	0.16 ± 0.01	0.17 ± 0.01	0.18 ± 0.001#	0.18 ± 0.01#	0.18 ± 0.02#	0.17 ± 0.01#

*p<0.05, #p<0.01 versus OVX

5. Histomorphometric analysis

Endocortical MAR was 20% greater in the group treated with 80μg/kg of hPTH(1-34), whereas periosteal MAR and BFR were 1- and 2-fold higher, respectively, in the $Ala^{1}Cys^{25}$hPTH(1-34) treated mice compared to OVX control mice (Table 2). Meanwhile, the lower dose of 40μg/kg of hPTH(1-34) or Cys^{25}hPTH(1-34) did not affect any of the dynamic histomorphometry measures.

Table 2. Histomorphometry parameters about bone formation

	Trabecular bone			Cortical bone					
	MS/BS [%]	MAR [mcm/day]	BFR/BS [mcm/day]	Ec.MAR [mcm/day]	Ec.M.Pm/ Ec.Pm[%]	Ec.BFR	Ps.MAR [mcm/day]	Ps.M.Pm /ps.Pm[%]	Ps.BFR
OVX	39.28 ± 13.10	3.80 ± 2.32	1.42 ± 0.56	1.004 ± 0.251	81.28 ± 14.13	0.839 ± 0.336	0.350 ± 0.388	15.51 ± 7.35	0.068 ± 0.091
hPTH(1-34)(40μg/kg)	37.50 ± 7.02	4.92 ± 2.97	1.98 ± 1.44	1.164 ± 0.280	64.90 ± 16.05	0.756 ± 0.253	0.416 ± 0.320	11.33 ± 10.13	0.067 ± 0.065
hPTH(1-34)(80μg/kg)	41.87 ± 8.11	5.64 ± 3.05	2.54 ± 1.44	1.266 ± 0.175*	77.85 ± 10.76	0.981 ± 0.166	0.778 ± 0.194	23.31 ± 8.17	0.190 ± 0.094*
Cys^{25}hPTH(1-34)	43.57 ± 15.77	3.77 ± 2.04	2.61 ± 3.09	0.950 ± 0.607	67.41 ± 24.49	0.736 ± 0.508	0.329 ± 0.297	10.81 ± 10.60	0.054 ± 0.075
$Ala^{1}Cys^{25}$hPTH(1-34)	40.72 ± 4.00	5.66 ± 3.10	2.34 ± 1.26	1.056 ± 0.479	60.03 ± 25.20	0.724 ± 0.384	0.757 ± 0.117*	25.47 ± 13.40	0.189 ± 0.106*

MAR, Mineral apposition rate; MS/BS, Mineralized surface/Bone surface; BFR, Bone formation rate; Ec, Endocortical; M.Pm, Mineralized perimeters; Ps, periosteal : *$p<0.05$ versus OVX

IV. DISCUSSION

In this study, we have showed that subcutaneously injecting Cys^{25}hPTH(1-34) analogues daily exerts significant anabolic effects on bone. We also observed that the anabolic effects of Cys^{25}hPTH(1-34) can be modified by a substitution of the first residue. Therefore, we propose Cys^{25}hPTH(1-34) analogues as a potential second generation PTH analogue for treating osteoporosis.

Teriparatide, human PTH(1-34) hormone, is the only bone anabolic agent that has been approved by the FDA for osteoporosis.[31] Most of its anabolic effects are through remodeling-based bone formation; however, some of the anabolic action of teriparatide is through modeling-based bone formation from the quiescent bone surface by activation of resting lining cells and/or recruitment of newly formed, differentiated osteoblasts to the bone surface.[32] Since PTH stimulates new bone formation, it has the potential to repair disordered bone architecture and increase bone mass.[33] However, one of the challenges with teriparatide has been the lack of early appreciable beneficial effects in nonvertebral fracture for at least the first 9 mo of treatment.[34] Teriparatide also does not increase hip BMD significantly more than alendronate.[35] Furthermore, in patients who have already been treated with oral bisphosphonates prior to teriparatide, the benefit of subsequent teriparatide treatment is diminished.[36] The anabolic effects of hPTH(1-34) are followed by excessive bone resorption. Increasing the dosage of PTH treatment is complicated, involving serious side effects of hypercalcemia and cortical porosity.[37,38] Therefore, new development of PTH or PTHrp analogues with purer anabolic activity, like Abaloparatide, is warranted.

In the present OVX mouse model experiments, we found that Cys^{25}hPTH(1-34) analogues exert anabolic effects on both trabecular and cortical bone in several parameters measured by μCT, while 40μg/kg injection of hPTH(1-34) did not. The differences between 80μg/kg and 40μg/kg group mice were considered to be related to dosage effects. The activity of cAMP generation with Cys^{25}hPTH(1-34) was lower than that of wild-type hPTH(1-34), and we confirmed the loss of sustained cAMP

response after the treatment of Cys^{25}hPTH(1-34) analogues. Lee et al. had reported that the mutated Cys^{25}hPTH(1-34) has a three-fold weaker binding affinity and cAMP generation with the loss of a sustained response.[26] Even though they had discussed whether the preferential binding to the RG or R^0 conformation of PTHR1 can induce a loss of sustained response of Cys^{25}hPTH(1-34), further study is needed. The development of hypocalcemia in the patient with homozygous mutation was also explained by the *in vivo* biological behavior of a weak agonist, Cys^{25}hPTH(1-84)[26]. Meanwhile, both the intra-cytoplasmic calcium signaling and ERK phosphorylation stimulated by Cys^{25}hPTH(1-34) analogues were comparable to those of wild-type hPTH(1-34) in this study. Therefore, we attempted to elucidate changes in BMD after the treatment with Cys^{25}hPTH(1-34) analogues *in vivo* as a kind of biased agonist, showing low cAMP generation and conserved β-arrestin-mediated signaling. In doing so, we showed that Cys^{25}hPTH(1-34) analogues contribute to anabolic effects on bone when injected subcutaneously once a day.

$DTrp^{12}$-PTH(7-34), a biased PTH that exhibits solely β-arrestin-mediated function, reportedly increased trabecular bone BMD significantly.[39,40] Meanwhile, hPTH(1-34) increased BMD in β-arrestin KO mice.[40] These results suggested that PKA signaling with β-arrestin-mediated signals plays a critical role in PTH-induced anabolic effects on bone. In a previous report, Bpa^1hPTH(1-34) lowered cAMP generation, while Ala^1hPTH(1-34) increased cAMP generation, compared to the hPTH(1-34).[9,41] When the first residue of Cys^{25}hPTH(1-34) was substituted with Ala^1 and Bpa^1 in this study, we observed changes in μCT parameters in both cortical and trabecular bone differed according to the first amino acid in the order of Ala^1Cys^{25}hPTH(1-34) = Cys^{25}hPTH(1-34) > Bpa^1Cys^{25}hPTH(1-34). Similarly, periosteal MAR and BFR increased with Ala^1Cys^{25}hPTH(1-34) treatment, even when compared to Cys^{25}hPTH(1-34) treatment. Thus, while Cys^{25}hPTH(1-34) tends to suppress periosteal bone remodeling compared to hPTH(1-34) (Cys^{25}hPTH(1-34) vs hPTH(1-34) $p<0.06$) for both Ps. MAR and Ps. BFR, Ala^1 may additionally stimulate bone formation. We suspect that the first amino acid in Csy^{25}hPTH(1-34) analogues

plays a critical role in bone anabolic effects.

Serum calcium levels increased as an acute response after subcutaneous injection of our PTH analogues, except the group exposed to a low dose of hPTH(1-34)(40μg/kg/d). Lee et al. also observed an increase in serum calcium just after subcutaneous injection of Cys^{25}hPTH(1-34) comparable to that achieved with hPTH(1-34) injection herein.[26] However, they showed that serum calcium levels reduced significantly after continuous infusion of Cys^{25}hPTH(1-34) with a much lower bone-resorption response.[29] Intermittent administration of Cys^{25}hPTH(1-34) may also benefit bone by suppressing bone resorption. When our PTH analogues were exposed to MC3T3E1 cells for 6 hours, the ratio of mRNA expression levels of RANKL/OPG ratio increased only in the hPTH(1-34) treated group. All of these findings suggest that the shallow bone resorption could be expected after a long term administration of Cys^{25}hPTH(1-34), as for Abaloparatide. The increase in trabecular and cortical bone observed by μCT despite similar dynamic histomorphometry measures in Cys^{25}hPTH(1-34) mice compared to control may be explained by suppressed osteoclastogenesis. Finally, the high BMD observed in the patient with an (Arg-to-Cys homozygous mutation at position 25 (R25C) could be partially explained as follows. Cys^{25}PTH(1-84) has a low cAMP generation capacity with a loss of sustained response, compared to wild-type PTH, which might suggest a preferential binding of Cys^{25} PTH(1-84) to the RG conformation of PTHR1, such as PTHrp or Abaloparatide. Therefore, compared to hPTH(1-34), Cys^{25}PTH(1-84) retains more pure anabolic activity with less bone resorption.

V. CONCLUSION

In conclusion, the high bone mass phenotype caused by an Arg to Cys mutation at the 25th residue of mature PTH(1-84), may be partially explained from direct and indirect effects exerted by the mutant PTH itself on bone. We also predict that Cys^{25}hPTH(1-34) derivatives would serve as a potential candidate as a second generation PTH analogue that improves both trabecular and cortical bone significantly with less hypocalcemia and less negative effects on cortical bone, such as cortical porosity.

REFERENCES

1. Swarthout JT, D'Alonzo RC, Selvamurugan N, Partridge NC. Parathyroid hormone-dependent signaling pathways regulating genes in bone cells. Gene. 2002;282(1-2):1-17.

2. Vilardaga JP, Romero G, Friedman PA, Gardella TJ. Molecular basis of parathyroid hormone receptor signaling and trafficking: a family B GPCR paradigm. Cell Mol Life Sci. 2011;68(1):1-13.

3. Ma YL, Zeng Q, Donley DW, Ste-Marie LG, Gallagher JC, Dalsky GP et al. Teriparatide increases bone formation in modeling and remodeling osteons and enhances IGF-II immunoreactivity in postmenopausal women with osteoporosis. J Bone Miner Res. 2006;21(6):855-64.

4. Saidak Z, Le Henaff C, Azzi S, Marty C, Marie PJ. Low-dose PTH increases osteoblast activity via decreased Mef2c/Sost in senescent osteopenic mice. J Endocrinol. 2014;223(1):25-33.

5. Esen E, Lee SY, Wice BM, Long F. PTH promotes bone anabolism by stimulating aerobic glycolysis via IGF signaling. J Bone Miner Res. 2015;30(11):1959-68.

6. Tregear GW, Van Rietschoten J, Greene E, Keutmann HT, Niall HD, Reit B et al. Bovine parathyroid hormone: minimum chain length of synthetic

peptide required for biological activity. Endocrinology. 1973;93(6):1349-53.

7. Kawai M, Mödder UI, Khosla S Rosen CJ. Emerging therapeutic opportunities for skeletal restoration. Nat Rev Drug Discov. 2011;10(2):141-56.

8. Gardella TJ, Wilson AK, Keutmann HT, Oberstein R, Potts JT Jr, Kronenberg M et al. Analysis of parathyroid hormone's principal receptor-binding region by site-directed mutagenesis and analog design. Endocrinology. 1993;132(5):2024-30.

9. Cupp ME, Nayak SK, Adem AS, Thomsen WJ. Parathyroid hormone (PTH) and PTH-related peptide domains contributing to activation of different PTH receptor-mediated signaling pathways. J Pharmacol Exp Ther. 2013;345(3):404-18.

10. Gesty-Palmer D, Chen M, Reiter E, Ahn S, Nelson CD, Wang S et al. Distinct beta-arrestin- and G protein-dependent pathways for parathyroid hormone receptor-stimulated ERK1/2 activation. J Biol Chem. 2006;281(16):10856-64.

11. Tilley DG. G protein-dependent and G protein-independent signaling pathways and their impact on cardiac function. Circ Res. 2011;109(2):217-30.

12. Luttrell LM, Lefkowitz RJ. The role of beta-arrestins in the termination and

transduction of G-protein-coupled receptor signals. J Cell Sci. 2002;115(Pt 3):455-65.

13. Defea K. Beta-arrestins and heterotrimeric G-proteins: collaborators and competitors in signal transduction. Br J Pharmacol. 2008;153 Suppl 1:S298-309.

14. Baillie GS, Sood A, McPhee I, Gall I, Perry SJ, Lefkowitz RJ et al. beta-arrestin-mediated PDE4 cAMP phosphodiesterase recruitment regulates beta-adrenoceptor switching from Gs to Gi. Proc Natl Acad Sci U S A. 2003;100(3):940-5.

15. Kobilka BK, Deupi X. Conformational complexity of G-protein-coupled receptors. Trends Pharmacol Sci. 2007 Aug;28(8):397-406.

16. Okazaki M, Ferrandon S, Vilardaga JP, Bouxsein ML, Potts JT Jr, Gardella TJ. Prolonged signaling at the parathyroid hormone receptor by peptide ligands targeted to a specific receptor conformation. Proc Natl Acad Sci U S A. 2008;105(43):16525-30.

17. Dean T, Vilardaga JP, Potts JT Jr, Gardella TJ. Altered selectivity of parathyroid hormone (PTH) and PTH-related protein (PTHrP) for distinct conformations of the PTH/PTHrP receptor. Mol Endocrinol. 2008 Jan;22(1):156-66.

18. Ferrandon S, Feinstein TN, Castro M, Wang B, Bouley R, Potts JT et al. Sustained cyclic AMP production by parathyroid hormone receptor endocytosis. Nat Chem Biol. 2009;5(10):734-42.

19. Hodsman AB, Fraher LJ, Watson PH, Ostbye T, Stitt LW, Adachi JD et al. A randomized controlled trial to compare the efficacy of cyclical parathyroid hormone versus cyclical parathyroid hormone and sequential calcitonin to improve bone mass in postmenopausal women with osteoporosis. J Clin Endocrinol Metab. 1997;82(2):620-8.

20. Black DM, Greenspan SL, Ensrud KE, Palermo L, McGowan JA, Lang TF et al. The effects of parathyroid hormone and alendronate alone or in combination in postmenopausal osteoporosis. N Engl J Med. 2003;349(13):1207-15.

21. Gafni RI, Brahim JS, Andreopoulou P, Bhattacharyya N, Kelly MH, Brillante BA et al. Daily parathyroid hormone 1-34 replacement therapy for hypoparathyroidism induces marked changes in bone turnover and structure. J Bone Miner Res. 2012;27(8):1811-20.

22. Leder BZ, O'Dea LS, Zanchetta JR, Kumar P, Banks K, McKay K et al. Effects of abaloparatide, a human parathyroid hormone-related peptide analog, on bone mineral density in postmenopausal women with osteoporosis. J Clin Endocrinol Metab. 2015;100(2):697-706.

23. Nakamura T, Sugimoto T, Nakano T, Kishimoto H, Ito M, Fukunaga M et al. Randomized Teriparatide [human parathyroid hormone (PTH) 1-34] Once-Weekly Efficacy Research (TOWER) trial for examining the reduction in new vertebral fractures in subjects with primary osteoporosis and high fracture risk. J Clin Endocrinol Metab. 2012;97(9):3097-106.

24. Thiruchelvam N, Randhawa J, Sadiek H, Kistangari G. Teriparatide induced delayed persistent hypercalcemia. Case Rep Endocrinol. 2014;2014:802473.

25. Hämmerle SP, Mindeholm L, Launonen A, Kiese B, Loeffler R, Harfst E et al. The single dose pharmacokinetic profile of a novel oral human parathyroid hormone formulation in healthy postmenopausal women. Bone. 2012;50(4):965-73.

26. Lee S, Mannstadt M, Guo J, Kim SM, Yi HS, Khatri A et al. A Homozygous [Cys25]PTH(1-84) Mutation That Impairs PTH/PTHrP Receptor Activation Defines a Novel Form of Hypoparathyroidism. J Bone Miner Res. 2015;30(10):1803-13.

27. Park HS, Han SH, Lee JY, Kim JE, Lim SK. Bone mineral density in patients with hypoparathyroidism. Paper presented at the 2015 Seoul International Congress of Endocrinology and Metabolism, Seoul, Korea; 2015.

28. Erben RG. Embedding of bone samples in methylmethacrylate: an improved method suitable for bone histomorphometry, histochemistry, and

immunohistochemistry. J Histochem Cytochem. 1997;45(2):307-13.

29. Dempster DW, Compston JE, Drezner MK, Glorieux FH, Kanis JA, Malluche H et al. Standardized nomenclature, symbols, and units for bone histomorphometry: a 2012 update of the report of the ASBMR Histomorphometry Nomenclature Committee. J Bone Miner Res. 2013;28(1):2-17.

30. Yang YM, Lee J, Jo H et al. Homer2 protein regulates plasma membrane Ca^{2+}-ATPase-mediated Ca^{2+} signaling in mouse parotid gland acinar cells. J Biol Chem. 2014;289(36):24971-9.

31. Shoback D. Update in osteoporosis and metabolic bone disorders. J Clin Endocrinol Metab. 2007;92(3):747-53.

32. Ma YL, Zeng Q, Donley DW, Ste-Marie LG, Gallagher JC, Dalsky GP et al. Teriparatide increases bone formation in modeling and remodeling osteons and enhances IGF-II immune reactivity in postmenopausal women with osteoporosis. J Bone Miner Res. 2006;21(6):855-64.

33. Chen P, Jerome CP, Burr DB, Turner CH, Ma YL, Rana A et al. Interrelationships between bone microarchitecture and strength in ovariectomized monkeys treated with teriparatide. J Bone Miner Res. 2007;22(6):841-8.

34. Krege JH, Wan X. Teriparatide and the risk of nonvertebral fractures in women with postmenopausal osteoporosis. Bone. 2012;50(1):161-4.

35. Saag KG, Zanchetta JR, Devogelaer JP, Adler RA, Eastell R, See K et al. Effects of teriparatide versus alendronate for treating glucocorticoid-induced osteoporosis: thirty-six-month results of a randomized, double-blind, controlled trial. Arthritis Rheum. 2009;60(11):3346-55.

36. Keel C, Kraenzlin ME, Kraenzlin CA, Müller B, Meier C. Impact of bisphosphonate wash-out prior to teriparatide therapy in clinical practice. J Bone Miner Metab. 2010;28(1):68-76.

37. Gafni RI, Guthrie LC, Kelly MH, Brillante BA, Christie CM, Reynolds JC et al. Transient Increased Calcium and Calcitriol Requirements after Discontinuation of Human Synthetic Parathyroid Hormone 1-34 (hPTH 1-34) Replacement Therapy in Hypoparathyroidism. J Bone Miner Res. 2015;30(11):2112-8.

38. Borba VZ, Mañas NC. The use of PTH in the treatment of osteoporosis. Arq Bras Endocrinol Metabol. 2010;54(2):213-9.

39. Qiu T, Wu X, Zhang F, Clemens TL, Wan M, Cao X. TGF-beta type II receptor phosphorylates PTH receptor to integrate bone remodeling signaling. Nat Cell Biol. 2010;12(3):224-34.

40. Gesty-Palmer D, Flannery P, Yuan L, Corsino L, Spurney R, Lefkowitz RJ et al. A beta-arrestin-biased agonist of the parathyroid hormone receptor (PTH1R) promotes bone formation independent of G protein activation. Sci Transl Med. 2009;1(1):1ra1.

41. Fiori N, Caporale A, Schievano E, Mammi S, Geyer A, Tremmel P et al. Structure-function relationship studies of PTH(1-11) analogues containing sterically hindered dipeptide mimetics. J Pept Sci. 2007;13(8):504-12.

ABSTRACT (IN KOREAN)

[Cys25]hPTH(1-34) 유도체의 생체 내 및 생체 외 효과

<지도교수 임 승 길>

연세대학교 대학원 의과학과

배 주 현

최근에 hPTH(1-84)의 25번째 아미노산이 Arginine에서 Cysteine으로 변형된 돌연변이가 부갑상선 기능 저하증의 한국인 환자에게서 보고되었다. 이 환자에게서 발견된 높은 골밀도가 부갑상선 기능 저하증 때문인지, 혹은 돌연변이 PTH의 증가 때문인지 명확히 하기 위하여 일련의 생체 내 및 생체 외 실험이 MC3T3E1, ROS 17/2.8 그리고 SAOS2세포에서 hPTH(1-34), Cys^{25}hPTH(1-34), $Ala^{1}Cys^{25}$hPTH(1-34) 그리고 $Bpa^{1}Cys^{25}$hPTH(1-34)의 펩타이드로 진행되었다.

hPTH(1-34) 과 $Ala^{1}Cys^{25}$hPTH(1-34)을 처리한 세포와 비교하였을 때, Cys^{25}hPTH(1-34) 혹은 $Bpa^{1}Cys^{25}$hPTH(1-34) 처리한 세포에서는 cAMP반응과 pCRE luciferase activity가 감소하였다. hPTH(1-34)를 MC3T3E1 세포에 처리하였을 때에는 cAMP의 반응이 지속되었지만, 다른 3가지 펩타이드 에서는 상기 반응이 관찰되지 않았다. 반면에, 모든 PTH 유도체들은 ERK의 인산화와 세포질 칼슘 신호에서 hPTH(1-34)와 유사한 결과를 보였다. OXV control 그룹과 비교하였을 때,

trabecular 와 cortical 뼈 부위는 6주간의 투여 후, 다음과 같은 순서로 증가하였다 : hPTH(1-34)(80㎍/kg) = $Ala^{1}Cys^{25}$hPTH(1-34)(80㎍/kg) = Cys^{25}hPTH(1-34)(80㎍/kg) > $Bpa^{1}Cys^{25}$hPTH(1-34)(80㎍/kg) > hPTH(1-34)(40㎍/kg). 6시간동안 Cys^{25}hPTH(1-34), $Ala^{1}Cys^{25}$hPTH(1-34) 그리고 $Bpa^{1}Cys^{25}$hPTH(1-34) 펩타이드를 처리하였을 때 RNAKL과 OPG의 mRNA비율은 hPTH(1-34)를 처리하였을 때보다 작았다. 결론적으로, hPTH(1-84)의 25번째 아미노산 부위에서 Arg 에서 Cys 로 돌연변이가 생긴 부갑상선 기능 저하증 환자에게서 발견된 높은 골밀도는 돌연변이 PTH가 직,간접적으로 뼈에 영향을 미쳤을 것으로 보이며 Cys^{25}hPTH(1-34)는 잠재적인 2세대 PTH 유도체가 될 가능성이 있다.

핵심되는 말: PTH유도체, 골다공증, 골형성